Circular photogalvanic effect on topological insulator surfaces: Berry-curvature-dependent response

Pavan Hosur

Phys. Rev. B **83**, 035309 — Published 18 January 2011

DOI: 10.1103/PhysRevB.83.035309

Circular photogalvanic-effect on topological insulator surfaces: Berry curvature-dependent response

Pavan Hosur
Department of Physics, University of California, Berkeley

We study theoretically the optical response of the surface states of a topological insulator, especially the generation of helicity-dependent direct current by circularly polarized light. Interestingly, the dominant current, due to an interband transition, is controlled by the Berry curvature of the surface bands. This extends the connection between photocurrents and Berry curvature beyond the quasiclassical approximation where it has been shown to hold. Explicit expressions are derived for the (111) surface of the topological insulator Bi_2Se_3 where we find significant helicity dependent photocurrents when the rotational symmetry of the surface is broken by an in-plane magnetic field or a strain. Moreover, the dominant current grows linearly with time until a scattering occurs, which provides a means for determining the scattering time. The dc spin generated on the surface is also dominated by a linear-in-time, Berry curvature dependent contribution.

PACS numbers:

I. INTRODUCTION

Topological insulators (TIs) have caught the eye of many a condensed matter physicist and materials scientist in recent years. In very simple terms, these are materials that have an insulating bulk but conducting surface states (SSs) that are protected against disorder by time-reversal symmetry. The reason for the tremendous amount of attention they have received is two-fold. One, they have been predicted to exhibit a number of exotic phenomena such as the magnetoelectric effect[1], magnetic monopole-like behavior[2] and the existence of topologically protected Majorana modes[3] with potential applications for topological quantum computing[4]. Two, a number of materials have already been theoretically predicted[5–9] and experimentally found[10–16] to be in this fascinating phase.

In their simplest incarnation, the SSs of TIs these correspond to the dispersion of a single Dirac particle, which cannot be realized in a purely two dimensional band structure with time reversal invariance. This dispersion is endowed with the property of spin-momentum locking, i.e., for each momentum there is a unique spin direction of the electron. Since several materials were theoretically predicted to be in this phase, most of the experimental focus on TIs so far has been towards trying to directly observe these exotic SSs in real or momentum space, in tunneling[10] and photoemission[11–16] experiments, respectively, and establish their special topological nature. However, there has so far been a dearth of experiments which study the response of these materials to external perturbations, such as an external electromagnetic field.

In order to fill this gap, we calculate here the response of TI surfaces to circularly polarized (CP) light. Since photons in CP light have a well-defined angular momentum, CP light can couple to the spin of the surface electrons. Then, because of the spin-momentum-locking feature of the SSs, this coupling can result in dc transport which is sensitive to the helicity (right- vs left-circular polarization) of the incident light. This phenomenon is known as the circular photogalvanic effect (CPGE). In this work, we derive general expressions for the direct current on a TI surface as a result of the CPGE at normal incidence within a two-band model and estimate its size for the (111) surface of Bi_2Se_3, an established TI, and find it to be well within measurable limits. Since bulk Bi_2Se_3 has inversion symmetry and the CPGE, which is a second-order non-linear effect, is forbidden for inversion symmetric systems, this current can only come from the surface.

We find, remarkably, that the dominant contribution to the current is controlled by the *Berry curvature* of the electron bands and *grows linearly with time*. In practice this growth is cut-off by a scattering event which resets the current to zero. At the microscopic level, this part of the current involves the absorption of a photon to promote an electron from the valence to the conduction band. The total current contains two other terms - both time-independent - one again involving an interband transition and the other resulting from intraband dynamics of electrons. However, for clean samples at low temperatures, the scattering or relaxation time is expected to be large, and these contributions will be eclipsed by the linear-in-time one. Hence, this experiment can also be used to measure the relaxation time for TI SSs.

Historically, the Berry curvature has been associated with fascinating phenomena such as the anomalous Hall effect[17] and the integer quantum Hall effect[18] and therefore, it is exciting that it appears in the response here. Its main implication here is that is gives us a simple rule, in addition to the requirement of the right symmetries, for identifying the perturbations that can give a linear-in-time CPGE at normal incidence: we look for perturbations that result in a non-zero Berry curvature. Put another way, we can identify perturbations that have the right symmetries

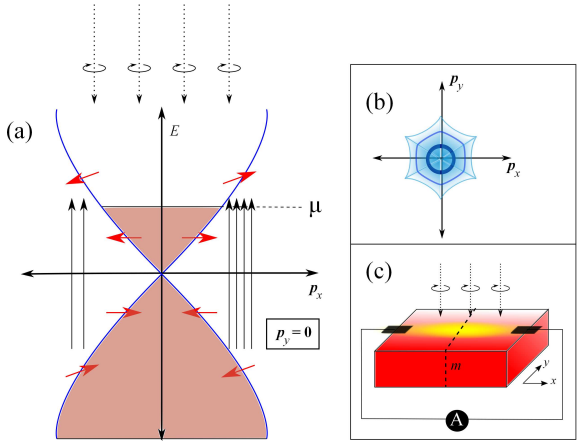

Figure 1: (Color online) (a) Schematic illustration of preferential absorption at one out of two points related by the reflection symmetry about the yz-plane. The short arrows denote the spin direction of electrons in various states. At low energies, the spins are completely in-plane. They acquire a small out-of-plane component at higher energies. The dotted lines represent incoming photons of helicity -1 (left-CP photons). These photons can only *raise* the $\langle S_z \rangle$ of an electron, and thus are preferentially absorbed by electrons whose $\langle S_z \rangle < 0$ in the valence band. The chemical potential μ must be between the initial and final states for any absorption to occur. (b) Constant energy contours for the surface conduction band of Bi_2Se_3. Dark lines denote lower energy. (a) is drawn at $p_y = 0$. (c) Geometry of the experiment. Light is incident normally on (111) surface of Bi_2Se_3. The dotted lines represent the mirror plane m about which the lattice has a reflection symmetry. The current $j_{a2}(t)$ (see text) is along $\hat{x}$.

but still do not give this current because the Berry curvature vanishes for these perturbations. Importantly, for TI SSs, the requirement of a non-zero Berry curvature amounts to the simple physical condition that the spin-direction of the electrons have all three components non-zero. In other words, if the electron spin in the SSs is completely in-plane, the Berry curvature is zero and no linear-in-time CPGE is expected. The spins must somehow be tipped slightly out of the plane, as shown in Fig. 1a, in order to get such a response. Thus, a pure Dirac (linear) dispersion, for which the spins are planar, cannot give this response; deviations from linearity, such as the hexagonal warping on the (111) surface of Bi_2Te_3[19], are essential for tilting the spins out of the plane.

CPGE has been observed in the past in GaAs[20], SiGe[21] and HgTe/CdHgTe[22] quantum wells - all systems with strong spin-orbit coupling. The effect in these systems can be understood within a four-band model consisting of two spin-orbit split valence bands and two spin-degenerate conduction bands. In contrast, TI SSs can be faithfully treated within a two-band model. The simplicity of the latter system makes it more convenient for studying theoretically compared to semiconductor quantum wells, and hence, enables us to determine a connection between the CPGE and the Berry curvature. In general, if a surface has no rotational symmetry about the surface normal, such a photocurrent is allowed.

Finally, we estimate the current on the (111) surface of Bi_2Se_3 using an effective model for the SSs[19,23]. This model captures the deviations from linearity of the SS dispersion due to the threefold rotational symmetry of the (111) surface of Bi_2Se_3. These deviations have been observed in photoemission experiments on Bi_2Te_3[11]. Similar deviations are expected for Bi_2Se_3[23], though they cannot be seen in the slightly smaller momentum range compared to Bi_2Te_3 over which data is currently available[24]. In order to get a direct current with CP light at normal incidence, rotational symmetry about the surface normal needs to be broken. Based on the requirement of non-zero Berry curvature, we propose to do this in two ways:

1. by applying an in-plane magnetic field and including deviations from linearity of the dispersion

2. by applying a strain.

With a magnetic field of $10T$ (With a 1% strain) and assuming a scattering time of $10ps$, (the scattering time in GaAs is $\sim 1ns$ over a wide range of temperatures[25]; we use a conservative estimate for Bi_2Se_3 here) we find that a current density of $\sim 100nA/mm$ ($\sim 10nA/mm$) can be obtained due to the CPGE with a 1Watt laser. This value can be easily measured by current experimental techniques. Conversely, the scattering time, crucial for transport processes, for Bi_2Se_3 SSs can be determined by measuring the current. In comparison, circular photogalvanic currents of a few nanoamperes per Watt of laser power have been measured in quantum wells of the semiconductors GaAs[20], SiGe[21] and HgTe/CdHgTe[22].

A connection between the optical response of a system and the Berry curvature of its bands has been previously noted at the low frequencies, where a semiclassical mechanism involving the anomalous velocity of electrons in a single band explains it[26,27]. Here, we show it for inter band transitions where no quasiclassical approximation is applicable. Instead, we calculate the quadratic response function directly. A connection is still present which points to a deeper relation between the response functions and the Berry curvature.

This paper is organized as follows. In Sec. II, we state the symmetry conditions under which a CPGE may occur. We present our results, both general as well as for Bi_2Se_3 in particular, in Sec. III A and describe the microscopic mechanism in Sec. III B. The calculation is described briefly in Sec. III C and in detail in Appendix B. In Sec. IV, we give our results for the optical injection of dc spin and in Sec. V we briefly discuss the situation where the rotational symmetry of the surface is broken by shining the light off-normally.

II. SYMMETRY CONSIDERATIONS FOR THE CPGE

In this section, we specify the symmetry conditions under which one can get a CPGE on the surface of a TI. But first, let us briefly review the concept of the CPGE in general.

The dominant dc response of matter to an oscillating electric field is, in general, quadratic in the electric field. When the response of interest is a current, the effect is known as the photogalvanic effect. This current can be written as

$$j_\alpha = \eta_{\alpha\beta\gamma}\mathcal{E}_\beta(\omega)\mathcal{E}_\gamma(-\omega) \tag{1}$$

where $\mathcal{E}_\alpha(t) = \mathcal{E}_\alpha(\omega)e^{i\omega t} + \mathcal{E}^*_\alpha(\omega)e^{-i\omega t}$ is the incident electric field, $\mathcal{E}^*_\alpha(\omega) = \mathcal{E}_\alpha(-\omega)$ and $\eta_{\alpha\beta\gamma}$ is a third rank tensor, which has non-zero components only for systems that break inversion symmetry, such as the surface of a crystal.

For j_α to be real, one has $\eta_{\alpha\beta\gamma} = \eta^*_{\alpha\gamma\beta}$. Thus, the real (imaginary) part of $\eta_{\alpha\beta\gamma}$ is symmetric (anti-symmetric) under interchange of β and γ, and therefore describes a current that is even (odd) under the transformation $\omega \to -\omega$. Consequently, j_α can be conveniently separated according to

$$j_\alpha = \mathtt{S}_{\alpha\beta\gamma}\left(\frac{\mathcal{E}_\beta(\omega)\mathcal{E}^*_\gamma(\omega) + \mathcal{E}^*_\beta(\omega)\mathcal{E}_\gamma(\omega)}{2}\right) + i\mathtt{A}_{\alpha\mu}(\boldsymbol{\mathcal{E}}\times\boldsymbol{\mathcal{E}}^*)_\mu \tag{2}$$

where $\mathtt{S}_{\alpha\beta\gamma}$ is the symmetric part of $\eta_{\alpha\beta\gamma}$ and $\mathtt{A}_{\alpha\mu}$ is a second-rank pseudo-tensor composed of the anti-symmetric part of $\eta_{\alpha\beta\gamma}$. For CP light, $\boldsymbol{\mathcal{E}} \propto \hat{x} \pm i\hat{y}$ if $\hat{z}$ is the propagation direction and only the second term in Eq. (2) survives, and hence represents the CPGE. This effect is odd in ω. On the other hand, the first term, which is even in ω, represents the linear photogalvanic effect as it is the only contribution for linearly polarized light. Since the transformation $\omega \to -\omega$, or equivalently, $\boldsymbol{\mathcal{E}} \to \boldsymbol{\mathcal{E}}^*$ reverses the helicity of CP light, i.e., changes right-CP light to left-CP light and vice versa, the CPGE is the helicity-dependent part of the photogalvanic effect.

The helicity of CP light is odd (i.e., right- and left-CP light get interchanged) under mirror reflection about a plane that contains the incident beam, but invariant under arbitrary rotation about the direction of propagation. Let us consider normal incidence of CP light on a TI surface normal to the z axis. Let us further assume that there is a mirror plane which is the y-z plane (See Fig. 1c). Then, the only component of direct current that reverses direction on switching the helicity is a current along the x axis. If there is also rotation symmetry R_z about the z-axis (such as the threefold rotation symmetry on the (111) surface of Bi_2Se_3), then no surface helicity-dependent direct photocurrent is permitted. One needs to break this rotation symmetry completely by applying, for example, and in-plane magnetic field, strain etc., to obtain a nonvanishing current.

III. HELICITY-DEPENDENT DIRECT PHOTOCURRENT

We now present our main results for the photocurrent and estimate it for Bi_2Se_3. After painting a simple microscopic picture for the mechanism, we give a brief outline of the full quantum mechanical treatment of the phenomenon.

A. Results

A general two-band Hamiltonian (in the absence of the incident light) can be written as

$$\mathbb{H} = \sum_{\mathbf{p}} c^\dagger_{\mathbf{p}} H_{\mathbf{p}} c_{\mathbf{p}} = \sum_{\mathbf{p}} |E_{\mathbf{p}}| c^\dagger_{\mathbf{p}} \hat{\mathbf{n}}(\mathbf{p}).\boldsymbol{\sigma} c_{\mathbf{p}} \tag{3}$$

upto a term proportional to the identity matrix, which is not important for our main result which involves only inter-band transitions. Here $\hat{\mathbf{n}}(\mathbf{p})$ is a unit vector, $\boldsymbol{\sigma}$ are the spin-Pauli matrices and $c_{\mathbf{p}} = (c_{\mathbf{p}\uparrow}, c_{\mathbf{p}\downarrow})^T$ is the electron annihilation operator spinor at momentum $\mathbf{p}$. Clearly, this can capture a Dirac dispersion, eg. with $E(\mathbf{p}) = \pm v_F p$ and $\hat{n}(\mathbf{p}) = v_F \hat{\mathbf{z}} \times \mathbf{p}$. It can also capture the SSs of Bi_2Se_3 in the vicinity of the Dirac point, which includes deviations beyond the Dirac limit. We also assume the Hamiltonian has a reflection symmetry m about y-axis, where $\hat{\mathbf{z}}$ is the surface normal. Using the zero temperature quadratic response theory described in Sec III C, we calculate the current due to the CPGE and find that

$$\vec{j}_{CPGE}(t) = (j_{na} + j_{a1} + j_{a2}(t))\,\hat{\mathbf{x}} \tag{4}$$

where the subscripts a (na) stand for "absorptive" and "non-absorptive", respectively. The absorptive part of the response involves a zero momentum interband transition between a pair of levels separated by energy $\hbar\omega$. These terms are only non zero when there is one occupied and one empty level. In this part of the response, we find a term that is time-dependent, $j_{a2}(t)$. In particular, this term grows linearly with the time over which the electromagnetic perturbation is present, which is allowed for a dc response. In reality, this linear growth is cut off by a decay process which equilibrates populations, and is characterized by a time constant τ. In clean samples at sufficiently low temperatures, characterized by large τ, this contribution is expected to dominate the response, and hence, is the focus of our work. The other contributions are discussed in Appendix B. Conversely, because of the linear growth with time, one can determine the lifetime of the excited states by measuring the photocurrent. This term is

$$j_{a2}(t) = -\frac{\pi e^3 \hbar \mathcal{E}_0^2 t \,\mathrm{sgn}(\omega)}{4} \sum_{\mathbf{p}} \delta(\hbar|\omega| - 2|E_{\mathbf{p}}|) v_x(\mathbf{p}) \mathcal{F}(\mathbf{p}) \tag{5}$$

where we have assumed that the chemical potential is in between the two energy levels $\pm|E_{\mathbf{p}}|$ connected by the optical frequency $\hbar\omega$, and that temperature can be neglected compared to this energy scale. Here, $v_x(\mathbf{p}) = \frac{\partial |E_{\mathbf{p}}|}{\partial p_x}$ is the conventional velocity and $\mathcal{F}(\mathbf{p}) = i \sum_{\mathbf{p}} \langle \partial_{p_x} u(\mathbf{p}) | \partial_{p_y} u(\mathbf{p}) \rangle + c.c.$, where $|u(\mathbf{p})\rangle$ is the conduction band Bloch state at momentum $\mathbf{p}$, is the *Berry curvature* of the conduction band at momentum $\mathbf{p}$. For the class of Hamiltonians (3) that we are concerned with, the Berry curvature is given by (See Appendix A):

$$\mathcal{F}(\mathbf{p}) = \hat{\mathbf{n}}.\left(\frac{\partial \hat{\mathbf{n}}}{\partial p_x} \times \frac{\partial \hat{\mathbf{n}}}{\partial p_y}\right) \tag{6}$$

which is the skyrmion density of the unit vector $\hat{\mathbf{n}}$ in momentum space. Since $\partial_{p_i} \hat{\mathbf{n}} \perp \hat{\mathbf{n}}$ for $i = x, y$, $\mathcal{F}(\mathbf{p}) \neq 0$ only if all three components of $\hat{\mathbf{n}}$ are nonvanishing. For linearly dispersing bands, $\hat{\mathbf{n}}$ has only two non-zero components (eg. $H_{\mathbf{p}} = p_y \sigma_x - p_x \sigma_y$, $\hat{\mathbf{n}} \propto (p_y, -p_x, 0)$). Hence, corrections beyond the pure Dirac dispersion are essential. Also, due to m, the Berry curvature satisfies $\mathcal{F}(p_x, p_y) = -\mathcal{F}(-p_x, p_y)$. Since in Eq. (5) we have the x-velocity multiplying the Berry curvature, which also transforms the same way, a finite contribution is obtained on doing the momentum sum.

We now calculate $j_{a2}(t)$ for the threefold-symmetric (111) surface of Bi_2Se_3 starting from the effective Hamiltonian[19,23]

$$H = v_F(p_x \sigma_y - p_y \sigma_x) + \frac{\lambda}{2}\left(p_+^3 + p_-^3\right)\sigma_z \tag{7}$$

where $v_F \sim 5 \times 10^5 m/s$[6] and $\lambda = 50.1 eV{\cdot}\text{Å}^3$[23]. A spin independent quadratic term has been dropped since it does not modify the answers for interband transitions, which only involve the energy difference between the bands.

To get a non-zero j_{CPGE}, the threefold rotational symmetry must be broken. We propose to do this in two separate ways:

1. **by applying a magnetic field B in the x-direction**
   This field has no orbital effect, and can be treated by adding a Zeeman term

   $$H'_{Zeeman} = -g_x \mu_B B \sigma_x \tag{8}$$

   , where g_x is the appropriate g-factor and μ_B is the Bohr magneton, to the Hamiltonian (7). To lowest order in λ and B, we get

   $$j_{a2}(t) = \frac{3 e^3 v_F \mathcal{E}_0^2 \lambda (g_x \mu_B B)^2 t}{16 \hbar^2 \omega} \mathcal{A} \tag{9}$$

   , where $\mathcal{A}$ is the laser spot-size. For $g_x = 0.5$[23], and assuming the experiment is done in a $10T$ field with a continuous wave laser with $\hbar\omega = 0.1eV$ which is less than the bulk band gap of $0.35eV$[13], $\mathcal{A} \sim 1mm^2$, a laser

power of $1W$, and the spin relaxation time $t \sim 10ps$, we get a current density of $\sim 100nA/mm$, which is easily measurable by current experimental techniques. Note that the expression (9) for $j_{a2}(t)$ contains the parameter λ which measures the coupling to σ_z in Eq. (7). Since $\vec{B} = B\hat{\mathbf{x}}$ breaks the rotation symmetry of the surface completely, a naive symmetry analysis suggests, wrongly, that deviations from linearity, measured by λ, are not needed to get $j_{a2}(t)$.

2. **by applying a strain along** x
This can be modeled by adding a term

$$H'_{strain} = \delta\lambda p_x^3 \sigma_z \tag{10}$$

to H in Eq. (7). This gives

$$j_{a2}(t) = \frac{3e^3 v_F(\delta\lambda)\mathcal{E}_0^2 \omega t}{2^7}\mathcal{A} \tag{11}$$

to lowest order in λ and $\delta\lambda$. For a 1% strain, $\delta\lambda/\lambda = 0.01$, and the same values for the other paramaters as in Eq.(9), we get a current density of $\sim 10nA/mm$. Eq. (11) does not contain λ; this is because $\delta\lambda$ alone both breaks the rotation symmetry and tips the spins out of the xy-plane.

B. Physical process

The appearance of the Berry curvature suggests a role of the anomalous velocity in generating the current. Such mechanisms have been discussed in the literature in the context of the CPGE[26,28]. However, those mechanisms only work when the electric field changes slowly compared to the typical scattering time. The SSs of Bi_2Se_3 probably have lifetimes of tens of picoseconds, and thus, we are in the opposite limit when $\hbar\omega = 0.1eV$, which corresponds to a time scale 10^3 times shorter.

In this limit, the dc responses are a result of a preferential absorption of the photon at one of the two momentum points for each pair of points $(\pm p_x, p_y)$ related by m, as shown in Fig. 1a for $p_y = 0$. According to the surface Hamiltonian (7), the spin vector $\mathbf{S} = \frac{\boldsymbol{\sigma}}{2}\hbar$ gets tipped out of the xy-plane for states that lie beyond the linear dispersion regime, but the direction of the tipping is opposite for (p_x, p_y) and $(-p_x, p_y)$. Thus, photons of helicity -1, which can only *raise* $\langle S_z\rangle$ of an electron, are preferentially absorbed by the electrons that have $\langle S_z\rangle < 0$ in the ground state. The response, then, is determined by the properties of these electrons. Clearly, the process is helicity-dependent as reversing the helicity would cause electrons with $\langle S_z\rangle > 0$ to absorb the light preferentially.

This is consistent with the requirement of a non-zero Berry curvature, which essentially amounts to the spin direction $\hat{\mathbf{n}}$ having to be a three-dimensional vector. In the linear limit, where $H = v_F(p_x\sigma_y - p_y\sigma_x)$, the spin is entirely in-plane, and all the electrons absorb the incident light equally.

C. Calculation in brief

We now briefly outline the calculation of the helicity-dependent photocurrent. The detailed calculation can be found in Appendix B. Readers only interested in our results may wish to skip this section.

The Model: The Hamiltonian and relevant electric field (vector potential) perturbations for getting a direct current to second order in the electric field of the incident photon are

$$H = |E_{\mathbf{p}}|\hat{\mathbf{n}}(p).\boldsymbol{\sigma} \tag{12}$$

$$H' = j_x A_x(t) + j_y A_y(t) \tag{13}$$

$$j_\alpha = \frac{\partial H}{\partial p_\alpha} \tag{14}$$

$$A_x(t) + iA_y(t) = A_0 e^{i(\omega - i\epsilon)t} \tag{15}$$

where $\mathbf{A}$ is the vector potential, $\hat{z}$ is assumed to be the surface normal, and ϵ is a small positive number which ensures slow switch-on of the light.

Quadratic response Theory: In general, the current along x to all orders in the perturbation H' is

$$\langle j_x\rangle(t) = \left\langle T^*\left(e^{i\int_{-\infty}^{t} dt' H'(t')}\right) j_x(t) T\left(e^{-i\int_{-\infty}^{t} dt' H'(t')}\right)\right\rangle \tag{16}$$

where T (T^*) denotes time-ordering (anti-time-ordering) and $O(t) = e^{iHt}Oe^{-iHt}$. Terms first order in H' cannot give a direct current. The contribution to the current from the second order terms can be written as

$$\langle j_x \rangle(t) = \int_{-\infty}^{t} dt' \int_{-\infty}^{t_1} dt'' \left\langle \left[\left[j_x(t), H'(t') \right], H'(t'') \right] \right\rangle$$
$$= \int_{-\infty}^{t} dt' \int_{-\infty}^{t_1} dt'' \chi_{x\alpha\beta}(t, t', t'') A_\alpha(t') A_\beta(t'') \quad (17)$$

where $\alpha, \beta \in \{x, y\}$, $\chi_{x\alpha\beta}(t, t', t'') = \chi_{x\alpha\beta}(0, t' - t, t'' - t) = \langle [[j_x, j_\alpha(t' - t)], j_\beta(t'' - t)] \rangle \equiv \chi_{x\alpha\beta}(t' - t, t'' - t)$ due to time translational invariance, and the expectation value is over the ground state which has all states with $E_{\mathbf{p}} < (>) 0$ filled (empty). For Hamiltonians of the form of Eq. (12), the expectation value of any traceless operator O in the Fermi sea ground state can be written as a trace:

$$\langle O \rangle = \sum_{\mathbf{p}} \frac{1}{2} \mathrm{Tr} \left\{ \left(1 - \frac{H}{|E_{\mathbf{p}}|} \right) O \right\} = - \sum_{\mathbf{p}} \frac{\mathrm{Tr}\,(HO)}{2|E_{\mathbf{p}}|} \quad (18)$$

This gives,

$$\chi_{x\alpha\beta}(t_1, t_2) = - \sum_{p} \frac{\mathrm{Tr}\,(H\,[[j_x, j_\alpha(t_1)]\,, j_\beta(t_2)])}{2|E_{\mathbf{p}}|} \quad (19)$$

Eq. (19) is the zero temperature limit of the finite temperature expression for the quadratic susceptibility proven in Ref.[29].

Because of the mirror symmetry m, $\chi_{x\alpha\beta}(t_1, t_2)$ is non-vanishing only for $\alpha \neq \beta$. To get a direct current, we retain only the non-oscillating part of $A_x(t + t_i)A_y(t + t_j) = \frac{A_0^2}{2} e^{2\epsilon t} \left[\sin\left(2\omega t + \omega(t_i + t_j)\right) - \sin\left(\omega(t_i - t_j)\right) \right]$. Thus,

$$j_x^{dc}(t) = \frac{A_0^2 e^{2\epsilon t}}{4} \int_{-\infty}^{0} dt_1 \int_{-\infty}^{t_1} dt_2 \Big\{ \left(\chi_{xxy} - \chi_{xyx} \right)(t_1, t_2) \times$$
$$e^{\epsilon(t_1 + t_2)} \sin\left(\omega(t_2 - t_1)\right) \Big\} \quad (20)$$

The Result: After carrying out the two time-integrals, we get the three currents mentioned in Eq. (4). For clean samples at low temperatures, $j_{a2}(t)$, which grows linearly with time, is expected to dominate. A general expression for this term is (in the units $e = \hbar = v_F = 1$ where v_F is the Fermi velocity)

$$j_{a2}(t) = \frac{i A_0^2 \pi t \mathrm{sgn}(\omega)}{2\omega^2} \sum_{\mathbf{p}} \delta(|\omega| - 2|E_{\mathbf{p}}|) \mathrm{Tr}(H j_x) \mathrm{Tr}(H [j_x, j_y]) \quad (21)$$

Using Eqs. (12) and (14) and the Lie algebra of the Pauli matrices, $[\sigma_i, \sigma_j] = 2i\epsilon_{ijk}\sigma_k$ where ϵ_{ijk} is the anti-symmetric tensor, the above traces can be written as

$$\mathrm{Tr}(H j_x) = 2|E_{\mathbf{p}}| v_x(\mathbf{p}) \quad (22)$$

$$\mathrm{Tr}(H\,[j_x, j_y]) = 4i|E_{\mathbf{p}}|^3 \hat{\mathbf{n}}.\left(\frac{\partial \hat{\mathbf{n}}}{\partial p_x} \times \frac{\partial \hat{\mathbf{n}}}{\partial p_y} \right)$$
$$= 4i|E_{\mathbf{p}}|^3 \mathcal{F}(\mathbf{p}) \quad (23)$$

Eqs. (21), (22) and (23) give our main result Eq. (5).

IV. OPTICAL SPIN INJECTION

Having understood the microscopic mechanism underlying the generation of the photocurrent $j_{a2}(t)$, we wonder, next, whether such a population imbalance can lead to any other helicity-dependent macroscopic responses. Since

each absorbed photon flips the z-component of the spin of an electron, a net $\langle S_z \rangle$ is expected to be generated on the surface. Such a process of optical spin injection was discussed for thin films of topological insulators[27], without, however, recognizing the role of the Berry curvature in the interband transition.

The calculation of $\langle S_z \rangle$ is identical to that of j_{CPGE}. The total $\langle S_z \rangle$ generated consists of the same three parts as j_{CPGE}, and the dominant part is

$$S^z_{a2}(t) = -\frac{\pi e^2 \mathcal{E}_0^2 \hbar t \mathrm{sgn}(\omega)}{8} \sum_{\mathbf{p}} \delta(\hbar|\omega| - 2|E_p|) n_z(\mathbf{p}) \mathcal{F}(\mathbf{p}) \tag{24}$$

S_z does not break the rotational symmetry of the surface, so we calculate $S^z_{a2}(t)$ directly for the threefold symmetric Hamiltonian (7) and obtain

$$S^z_{a2}(t) = \frac{e^2 \mathcal{E}_0^2 (\hbar\omega)^3 \lambda^2 t}{2^{10}} \mathcal{A} \tag{25}$$

For the same values of all the parameters as for $j_{a2}(t)$, we get $S^z_{a2}(t) \sim 10\hbar$, which means only ten electron spins are flipped over an area of $\sim 1mm^2$. This is a very small number and cannot be measured by the current experimental techniques. However, the result that the dominant spin injected onto the surface is also controlled by the Berry curvature is still theoretically interesting, as it points towards a deeper connection between the Berry curvature of electron bands and the helicity-dependent dc responses of systems with strong spin-orbit coupled coupling.

V. CPGE AT OBLIQUE INCIDENCE

Experimentally, a very attractive way of breaking the rotational symmetry of the surface is by performing the experiment with obliquely incident light. Indeed, such experiments have already been performed successfully on graphene at low frequencies[31]. At the microscopic level, the effect there has been attributed to photon-drag, where the current arises as a result of the in-plane component of the photon momentum $q_\parallel$ getting transferred to the electrons in graphene. In general, an analogous process is expected to contribute to the CPGE at high-frequencies as well. We can estimate the size of the photon-drag effect on TI surfaces in the Dirac limit by considering a mechanism is similar to the one described in Sec. III B, i.e., the electrons at $(\pm p_x, p_y)$ absorb the incident light unequally if the light is incident in the yz-plane. Now, no out-of-plane tipping of the spin is needed, because, if one thinks of the helical photon as simply a spin-raising or lowering operator for spins parallel to its propogation direction $\hat{\mathbf{z}}'$, the electrons at $(\pm p_x, p_y)$ already have opposite $\langle S_{z'} \rangle$ and hence, will absorb the light unequally. Thus, the general expression for the current may contain only those material parameters which appear in the pure Dirac dispersion. As before, it must be quadratic in the photon electric field, and must change sign when $q_\parallel$ and ω are both reversed, since that corresponds to switching the photon helicity. Thus, to lowest order in $q_\parallel$, the linear-in-time current, based simply on symmetry and dimensional analysis, must be of the form

$$\vec{\mathbf{j}}_{photon-drag}(t) \sim \frac{e^3 E_0^2 v_F^2 q_\parallel t}{\hbar^2 \omega^2} \mathcal{A} \hat{\mathbf{x}} \tag{26}$$

For $q_\parallel = c/\omega$, c being the speed of light in vacuum, and the same values for all the other parameters as in Sec. III A, we get a current density of $\sim 1\mu A/mm$. This will dominate the response at off-normal incidence, but can be suppressed by careful alignment of the experimental setup. However, since a response might appear even in the pure Dirac limit in which the Berry curvature vanishes, the role of the Berry curvature is not clear for this process.

In graphene, helicity-dependent direct photocurrents have also been predicted by applying a dc bias[30]. However, with a dc bias across a TI surface and ordinary continuous lasers, we find the current to be too low to be measurable.

VI. CONCLUSIONS

In summary, we studied the CPGE on the surface of a TI at normal incidence, and applied the results to the (111) surface of Bi_2Se_3. If the rotational symmetry of the TI surface is broken by applying an in-plane magnetic field or a strain, we predict an experimentally measurable direct photocurrent. A striking feature of this current is that it depends on the Berry curvature of the electron bands. Such a dependence can be understood intuitively as a result of the incident photons getting absorbed unequally by electrons of different momenta and hence, different average spins. The current grows linearly with time until a decay process equilibrates populations, which provides a way of determining the excited states lifetime. We also calculated the amount of dc helicity-dependent out-of-plane

component of the electron spin generated. This does not require any rotational symmetry breaking; however, the numerical value is rather small with typical values of the parameters. Finally, we estimated the size of the CPGE due to the photon-drag effect at oblique incidence assuming a differential absorption mechanism similar to the one discussed for normal incidence, and found a rather large value. However, the role of the Berry curvature in this process was unclear.

For future work, we wonder whether the Berry curvature dependence of the helicity-dependent response to CP light survives for three- and higher-band models. This is a practically relevant question, as semiconductor quantum wells such as those of GaAs, SiGe and HgTe/CdHgTe demand a four-band model for modeling the CPGE.

We would like to thank Ashvin Vishwanath for enlightening discussions, Joseph Orenstein for useful experimental inputs, and Ashvin Vishwanath and Yi Zhang for invaluable feedback on the draft.

This work was supported by the Office of Basic Energy Sciences, Materials Sciences Division of the U.S. Department of Energy under contract No. DE-AC02-05CH1123.

Appendix A: Proof of Berry curvature expression

Here we show that the Berry curvature defined for Bloch electrons as

$$\mathcal{F}(\mathbf{p}) = i\left(\langle\partial_{p_x}u|\partial_{p_y}u\rangle - \langle\partial_{p_y}u|\partial_{p_x}u\rangle\right) \tag{A1}$$

can be written as

$$\mathcal{F}(\mathbf{p}) = \hat{\mathbf{n}}.\left(\partial_{p_x}\hat{\mathbf{n}}\times\partial_{p_y}\hat{\mathbf{n}}\right) \tag{A2}$$

for the band with energy $|E_{\mathbf{p}}|$ for Hamiltonians of the form $H_{\mathbf{p}} = |E_{\mathbf{p}}|\hat{\mathbf{n}}(\mathbf{p}).\boldsymbol{\sigma}$.

At momentum $\mathbf{p}$, the Bloch state $|u_{\mathbf{p}}\rangle$ with energy $|E_{\mathbf{p}}|$ is defined as the state whose spin is along $\hat{\mathbf{n}}(\mathbf{p})$. Defining $|\uparrow\rangle$ as the state whose spin is along $+\hat{\mathbf{z}}$, $|u_{\mathbf{p}}\rangle$ is obtained by performing the appropriate rotations,

$$|u_{\mathbf{p}}\rangle = e^{-i\frac{\sigma_z}{2}\phi(\mathbf{p})}e^{i\frac{\sigma_y}{2}\theta(\mathbf{p})}|\uparrow\rangle \tag{A3}$$

where $\theta(\mathbf{p})$ and $\phi(\mathbf{p})$ are the polar angles that define $\hat{\mathbf{n}}(\mathbf{p})$:

$$\hat{\mathbf{n}}(\mathbf{p}) = \sin\theta(\mathbf{p})\cos\phi(\mathbf{p})\hat{x} + \sin\theta(\mathbf{p})\sin\phi(\mathbf{p})\hat{y} + \cos\theta(\mathbf{p})\hat{z} \tag{A4}$$

Substituting Eq. (A3) in Eq. (A1), one gets

$$\mathcal{F}(\mathbf{p}) = \sin\theta(\mathbf{p})\left(\partial_{p_x}\theta(\mathbf{p})\partial_{p_y}\phi(\mathbf{p}) - \partial_{p_x}\phi(\mathbf{p})\partial_{p_y}\theta(\mathbf{p})\right) \tag{A5}$$

which, on using Eq. (A4) and some algebra, reduces to the required expression Eq. (A2).

Appendix B: current calculation for the cpge

Here we explain the current-calculation of Sec. III A in more detail and also state results for the parts of the current that we chose not to focus on there.

As shown in Sec. III C, the relevant susceptibility is

$$\begin{aligned}\chi^{x\alpha\beta}(t,t',t'') &= -\frac{1}{2}\sum_{\mathbf{p}}\mathrm{Tr}\left(\frac{H}{|E_{\mathbf{p}}|}\left[[j^x(t),j^\alpha(t')],j^\beta(t'')\right]\right)\\ &= -\sum_{\mathbf{p}}\frac{1}{2|E_{\mathbf{p}}|}\mathrm{Tr}\left(H\left[[j^x,j^\alpha(t_1)],j^\beta(t_2)\right]\right)\\ &\equiv \chi^{x\alpha\beta}(t_1,t_2)\end{aligned} \tag{B1}$$

where $t_1 = t'-t$, $t_2 = t''-t$, and the non-vanishing components of $\chi^{x\alpha\beta}$ are those for which $\alpha\neq\beta$. The non-oscillating part of the current, hence, is

$$\langle j_x^{dc}\rangle(t) = j_{CPGE}(t) = \frac{A_0^2e^{2\epsilon t}}{4}\int_{-\infty}^{0}dt_1\int_{-\infty}^{t_1}dt_2 \left(\chi^{xxy}(t_1,t_2) - \chi^{xyx}(t_1,t_2)\right)e^{\epsilon(t_1+t_2)}\sin\left(\omega(t_2-t_1)\right) \tag{B2}$$

Since $j_{CPGE}(t)$ is an odd function of ω, it reverses on reversing the polarization, as expected.

The traces in the susceptibility expressions are calculated by introducing a complete set of states in place of the identity several times. Thus,

$$\begin{aligned}
&\chi^{xxy}(t_1,t_2) \qquad\qquad (B3)\\
&=-\sum_{\mathbf{p}}\frac{1}{2|E_{\mathbf{p}}|}\mathrm{Tr}\left(H\left[[j^x,j^x(t_1)],j^y(t_2)\right]\right)\\
&=-\frac{1}{2}\sum_{\mathbf{p}}\sum_{nml}\mathrm{sgn}(E_n)\Big\{e^{i(E_m-E_n)t_2}\times\\
&\left(e^{i(E_l-E_m)t_1}-e^{-i(E_l-E_n)t_1}\right)X_{nl}X_{lm}Y_{mn}+\text{c.c.}\Big\}
\end{aligned}$$

where $X_{nl}=\langle n\,|j_x|\,m\rangle$ etc. and the subscript $\mathbf{p}$ on $E_{\mathbf{p}}$ has been dropped to enhance the readability. Similarly,

$$\begin{aligned}
&\chi^{xyx}(t_1,t_2) \qquad\qquad (B4)\\
&=-\sum_{\mathbf{p}}\frac{1}{2E_{\mathbf{p}}}\mathrm{Tr}\left(H\left[[j^x,j^y(t_1)],j^x(t_2)\right]\right)\\
&=-\frac{1}{2}\sum_{\mathbf{p}}\sum_{nml}\mathrm{sgn}(E_n)\Big\{e^{i(E_m-E_n)t_2}X_{mn}\times\\
&\left(e^{i(E_l-E_m)t_1}X_{nl}Y_{lm}-e^{-i(E_l-E_n)t_1}Y_{nl}X_{lm}\right)+\text{c.c.}\Big\}
\end{aligned}$$

Substituting (B3) and (B4) in (20), we get

$$\begin{aligned}
&j_{CPGE}(t)=\frac{A_0^2e^{2\epsilon t}}{4}\mathfrak{Re}\int_{-\infty}^{0}dt_1\int_{-\infty}^{t_1}dt_2e^{\epsilon(t_1+t_2)}\times \qquad (B5)\\
&\sin\left(\omega(t_1-t_2)\right)\sum_{\mathbf{p},nml}\mathrm{sgn}(E_n)e^{i(E_m-E_n)t_2}\times\\
&\Big\{\left(e^{i(E_l-E_m)t_1}-e^{-i(E_l-E_n)t_1}\right)X_{nl}X_{lm}Y_{mn}-\\
&X_{mn}\left(e^{i(E_l-E_m)t_1}X_{nl}Y_{lm}-e^{-i(E_l-E_n)t_1}Y_{nl}X_{lm}\right)\Big\}
\end{aligned}$$

where $\mathfrak{Re}$ stands for 'the real part of'. Carrying out the the two time integrations gives

$$\begin{aligned}
&j_{CPGE}(t)=\frac{A_0^2e^{2\epsilon t}}{8}\mathfrak{Im}\sum_{\mathbf{p}}\sum_{nml}\mathrm{sgn}(E_n)\times \qquad (B6)\\
&\left[\frac{1}{E_m-E_n+\omega-i\epsilon}-\frac{1}{E_m-E_n-\omega-i\epsilon}\right]\times\\
&\left\{\frac{X_{nl}\left(X_{lm}Y_{mn}-Y_{lm}X_{mn}\right)}{E_l-E_n-2i\epsilon}+\frac{X_{lm}\left(Y_{mn}X_{nl}-X_{mn}Y_{nl}\right)}{E_l-E_m+2i\epsilon}\right\}
\end{aligned}$$

where $\mathfrak{Im}$ stands for 'the imaginary part of'. Using $\mathfrak{Im}\left(\frac{1}{\Omega-i\epsilon}\right)=\pi\delta(\Omega)$ and $\mathfrak{Re}\left(\frac{1}{\Omega-i\epsilon}\right)=\frac{1}{\Omega}$ in the limit $\epsilon\to 0$, we get after some algebra, $j_{CPGE}(t)=j_{na}+j_{a1}+j_{a2}(t)$, where (Tr denotes the trace)

$$\begin{aligned}
j_{na}&=\frac{A_0^2}{16}\sum_{\mathbf{p}}\frac{\omega(\omega^2-12E_{\mathbf{p}}^2)}{i|E_{\mathbf{p}}|^3(\omega^2-4E_{\mathbf{p}}^2)^2}\times\\
&\mathrm{Tr}(Hj_x)\mathrm{Tr}(H\left[j_x,j_y\right]) \qquad (B7)
\end{aligned}$$

comes from intraband processes and is constant in time,

$$\begin{aligned}
j_{a1}&=-\frac{\pi A_0^2\mathrm{sgn}(\omega)}{32}\sum_{\mathbf{p}}\frac{\delta(|\omega|-2|E_{\mathbf{p}}|)}{E_{\mathbf{p}}^2}\times\\
&\mathrm{Tr}(H\left[j_x,[j_x,j_y]\right]) \qquad (B8)
\end{aligned}$$

is a result of an interband transition absorption as indicated by the δ-function in energy and is also constant in time, and

$$j_{a2}(t) = i\frac{A_0^2 \pi t\, \mathrm{sgn}(\omega)}{8} \sum_p \delta(|\omega| - 2|E_{\mathbf{p}}|) \times \frac{\mathrm{Tr}(H j_x)\mathrm{Tr}(H\,[j_x, j_y])}{E_{\mathbf{p}}^2} \tag{B9}$$

which also results from interband absorption and increases linearly in time. The last term was the main focus of our work.

[1] Essin, A. M., Moore, J. E. & Vanderbilt, D. Magnetoelectric polarizability and axion electrodynamics in crystalline insulators. Phys. Rev. Lett. 102, 146805 (2009).
[2] Qi, X.-L. et al. Inducing a magnetic monopole with topological surface states. Science 323, 1184–1187 (2009).
[3] Fu, L. & Kane, C. L. Superconducting proximity effect and Majorana fermions at the surface of a topological insulator. Phys. Rev. Lett. 100, 096407 (2008).
[4] Collins, G. P. Computing with quantum knots. Sci. Am. 294, 57–63 (2006).
[5] L. Fu and C. L. Kane, Phys. Rev. B 76, 045302 (2007).
[6] H. Zhang, C. X. Liu, X. L. Qi, X. Dai, Z. Fang, S. C. Zhang, Nature Physics 5, 438 (2009).
[7] Binghai Yan, Chao-Xing Liu, Hai-Jun Zhang, Chi-Yung Yam, Xiao-Liang Qi, Thomas Frauenheim, Shou-Cheng Zhang, arXiv:1003.0074.
[8] S. Chadov, X.-L. Qi, J Kübler, G. H. Fecher, C. Felser, S.-C. Zhang, arXiv:1003.0193.
[9] Binghai Yan, Hai-Jun Zhang, Chao-Xing Liu, Xiao-Liang Qi, Thomas Frauenheim, Shou-Cheng Zhang, arXiv:1008.2241.
[10] P. Roushan, J. Seo, C. V. Parker, Y. S. Hor, D. Hsieh, D. Qian, A. Richardella, M. Z. Hasan, R. J. Cava, A. Yazdani, Nature 460, 1106-1109 (2009).
[11] Y. L. Chen, J. G. Analytis, J. H. Chu, Z. K. Liu, S. K. Mo, X. L. Qi, H. J. Zhang, D. H. Lu, X. Dai, Z. Fang, S. C. Zhang, I. R. Fisher, Z. Hussain, Z. X. Shen, Science Vol. 325 no. 5937, pp178 (2009).
[12] D. Hsieh, D. Qian, L. Wray, Y. Xia, Y. Hor, R. J. Cava, and M. Z. Hasan, Nature **452**, 970 (2008).
[13] Y. Xia, L. Wray, D. Qian, D. Hsieh, A. Pal, H. Lin, A. Bansil, D. Grauer, Y. S. Hor, R. J. Cava, M. Z. Hasan, Nat. Phy. Vol. 5, No. 6, pp398 (2009).
[14] H. Lin, L.A. Wray, Y. Xia, S. Jia, R.J. Cava, A. Bansil, M.Z. Hasan, arXiv:1003.0155.
[15] H. Lin, R.S. Markiewicz, L.A. Wray, L. Fu, M.Z. Hasan, A. Bansil, arXiv:1003.2615.
[16] Takafumi Sato, Kouji Segawa, Hua Guo, Katsuaki Sugawara, Seigo Souma, Takashi Takahashi, Yoichi Ando, arXiv:1006.2437.
[17] F. D. M. Haldane, Phys. Rev. Lett. 93, 206602 (2004).
[18] D. J. Thouless, M. Kohmoto, M. P. Nightingale, M. denNijs, Phys. Rev. Lett. 49, 405 (1982).
[19] L. Fu, Phys. Rev. Lett. 103, 266801 (2009).
[20] S. D. Ganichev, E. L. Ivchenko, S. N. Danilov, J. Eroms, W. Wegscheider, D. Weiss, and W. Prettl , Phys. Rev. Lett. 86, 4358 (2001).
[21] S. D. Ganichev, F. P. Kalz, U. Rossler, W. Prettl, E. L. Ivchenko, V. V. Bel 'kov, R. Neumann, K. Brunner, G. Abstreiter, Mat. Res. Soc. Symp. Proc. Vol. 690, F3.11.1 (2002).
[22] B. Wittmann, S. N. Danilov, V. V. Bel'kov, S. A. Tarasenko, E. G. Novik, H. Buhmann, C. Brune, L. W. Molenkamp, Z. D. Kvon, N. N. Mikhailov, S. A. Dvoretsky, N. Q.Vinh, A. F. G. van der Meer, B. Murdin, and S. D. Ganichev, arXiv:1002.2528v1.
[23] Chao-Xing Liu, Xiao-Liang Qi, HaiJun Zhang, Xi Dai, Zhong Fang, Shou-Cheng Zhang, arXiv:1005.1682.
[24] D. Hsieh, Y. Xia, D. Qian, L. Wray, J. H. Dil, F. Meier, J. Osterwalder, L. Patthey, J. G. Checkelsky, N. P. Ong, A. V. Fedorov, H. Lin, A. Bansil, D. Grauer, Y. S. Hor, R. J. Cava & M. Z. Hasan, Nature 460, 1101 (2009).
[25] L. Munoz, E. Perez, L. Vina, K. Ploog, Phys. Rev. B 51, 4247 (1995).
[26] E. Deyo, L. E. Golub, E. L. Ivchenko, B. Spivak, arXiv:0904.1917v1.
[27] H. Z. Lu, W. Y. Shan, W. Yao, Q. Niu, S. Q. Shen, Phys. Rev. B 81, 115407 (2010).
[28] J. E. Moore, J. Orenstein, arXiv:0911.3630v1.
[29] Ch. 7, 'Nonlinear Optical Phenomena', Paul N. Butcher, Eq. 7.25 and preceding discussion.
[30] T. Oka, H. Aoki, Phys. Rev. B 79, 081406(R), 2009.
[31] J. Karch, P. Olbrich, M. Schmalzbauer, C. Brinsteiner, U. Wurstbauer, M.M. Glazov, S.A. Tarasenko, E.L. Ivchenko, D. Weiss, J. Eroms, S.D. Ganichev, arXiv:1002.1047v1.
[32] N. P. Ong, W. L. Lee, Foundations of Quantum Mechanics, ed. Sachio Ishioka and Kazuo Fujikawa (World Scientific, 2006), p. 121.